

# Immunostimulatory TLR7 Agonist-Nanoparticles Together with Checkpoint Blockade for Effective Cancer Immunotherapy

Ching-Hsin Huang, Natalie Mendez, Oscar Hernandez Echeagaray, Joi Weeks, James Wang, Shiyin Yao, Sarah L. Blair, Natalie Gude, William C. Trogler, Dennis A. Carson, Tomoko Hayashi,\* and Andrew C. Kummel\*

**Mono- or dual-checkpoint inhibitors for immunotherapy have changed the paradigm of cancer care; however, only a minority of patients responds to such treatment. Combining small molecule immunostimulators can improve treatment efficacy, but they are restricted by poor pharmacokinetics. In this study, conjugated TLR7 agonists onto silica nanoparticles show extended drug localization after intratumoral injection. The nanoparticle-based TLR7 agonist increases immune stimulation by activating the TLR7 signaling pathway. When treating CT26 colon cancer, nanoparticle conjugated TLR7 agonists increase T cell infiltration into the tumors by >4× and upregulate expression of the interferon  $\gamma$  gene compared to its unconjugated counterpart by  $\approx 2\times$ . Toxicity assays establish that the conjugated TLR7 agonist is a safe agent at the effective dose. When combined with checkpoint inhibitors that target programmed cell death protein 1 (PD-1) and cytotoxic T-lymphocyte-associated protein 4 (CTLA-4), a 10–100× increase in immune cell migration is observed; furthermore, 100 mm<sup>3</sup> tumors are treated, and a 60% remission rate is observed including remission at contralateral noninjected tumors. The data show that nanoparticle-based TLR7 agonists are safe and can potentiate the effectiveness of checkpoint inhibitors in immunotherapy resistant tumor models and promote a long-term specific memory immune function.**

Colorectal cancer (CRC) is one of the top three causes of cancer death worldwide, it is currently being investigated for immunotherapy.<sup>[1]</sup> Metastatic CRC (mCRC) patients usually receive systemic therapy, such as anti-VEGF or anti-EGFR, but often this results in acquired resistance.<sup>[1,2]</sup> The checkpoint inhibitor antibodies, targeting programmed cell death protein 1 (a-PD-1) and cytotoxic T-lymphocyte-associated protein 4 (a-CTLA-4), block the inhibitory signals between T cells/tumor cells and T cells/antigen presenting cells (APC) and have shown promising therapeutic effects (Scheme S1, Supplementary Information). Checkpoint inhibitors, such as ipilimumab (a-CTLA-4 antibody) and nivolumab (a-PD-1 antibody), improve outcomes for many tumors, which include melanoma, advanced lung, and head and neck cancers. They are also being evaluated to treat mCRC patients.<sup>[3]</sup> However, a large portion of patients, including the majority of mCRC patients, do not respond to immune checkpoint inhibitors.<sup>[4–6]</sup>

Data from current clinical trials indicate that patients whose tumors are mismatch repair deficient (MMRd) are likely to respond to checkpoint inhibitor therapies.<sup>[7–9]</sup> It has been postulated that the DNA mismatch repair deficiency leads to more neoantigens released that are easily recognized by the body's immune cells to induce tumor-specific immune response. Pembrolizumab (a-PD-1 drug) has recently been designated by the US Food and Drug Administration (FDA) for use in MMRd tumors, regardless of the tumor location.<sup>[10]</sup> Even though immune checkpoint inhibitors have shown great promise for many cancer patients, mismatch repair proficient (MMRp) cancer patients are less responsive.<sup>[9,11]</sup> Even in MMRd mCRC, the objective response rate is about 40%.<sup>[12]</sup> Checkpoint inhibitors are not effective in MMRp mCRC<sup>[12]</sup> consistent with MMRp cancers having lower lymphocyte infiltration into tumors.<sup>[7]</sup> Therefore, rendering these tumors sensitive to immunotherapy remains a major challenge,<sup>[6]</sup> and using immunostimulatory agents could be a complementary approach to

C.-H. Huang, Dr. N. Mendez, Dr. J. Wang, Prof. W. C. Trogler, Prof. A. C. Kummel  
Department of Chemistry & Department of Medicine  
University of California, San Diego  
9500 Gilman Drive, La Jolla, San Diego, CA 92093, USA  
E-mail: akummel@ucsd.edu

O. H. Echeagaray, J. Weeks, Prof. N. Gude  
Molecular Biology Institute  
San Diego State University  
5500 Campanile Drive, San Diego, CA 92182, USA

S. Yao, Dr. S. L. Blair, Prof. D. A. Carson, Dr. T. Hayashi  
Moore's Cancer Center  
University of California, San Diego  
3855 Health Sciences Drive, La Jolla, CA 92037, USA  
E-mail: thayashi@ucsd.edu

 The ORCID identification number(s) for the author(s) of this article can be found under <https://doi.org/10.1002/adtp.201900200>

DOI: 10.1002/adtp.201900200

improve cancer treatment with checkpoint inhibitors. Murine colon cancer cell line, CT26, one of the most extensively used syngeneic mouse tumor models that lack mutations in mismatch repair genes,<sup>[13-15]</sup> was chosen for the present study.

A previously synthesized nanoparticle-based immunostimulatory agent, which consists of a TLR7 agonist (TLR7a) conjugated with 100 nm silica nanoshells (NS) termed NS-TLR7a (agonist number per nanoshell is 6000 or greater),<sup>[16]</sup> has shown improved TLR7 immune adjuvant activity.<sup>[16]</sup> NS-TLR7a increased cytokine IL-12 secretion and activated the inflammasome pathway in mouse dendritic cells (DCs).<sup>[16]</sup> Furthermore, NS-TLR7a enhanced a Th1-biased immune response that is often associated with induction of cytotoxic T lymphocytes (CTL)<sup>[16]</sup> that play a critical role in cancer immunotherapy because they recognize and kill cancerous cells.<sup>[17]</sup> In the present study, NS-TLR7a was used to amplify the immune response combined with checkpoint inhibitors to restore the T lymphocytes' killing capability in an animal model. Such combination therapy has the potential to treat MMRp patients by developing tumor antigen-specific T cells at both the tumor site and systemically. Nanoparticle-based TLR7/8 agonists were used in a combination treatment strategy similar to previous studies, as shown in Table S2 (Supporting Information). Most previous studies lacked investigation of potential immune-related adverse effects and other systemic toxicity, which is a critical problem with potent immunostimulating drugs.<sup>[18,19]</sup> Some previous studies used known tumor antigens to induce and amplify the immune response,<sup>[20]</sup> but identifying the neoantigens accounting for immune responses of spontaneous tumors is very challenging.<sup>[21]</sup> Furthermore, most focused on local control of tumor growth and did not address the potential of systemic immune responses and tumor progression at distal sites.<sup>[20,22,23]</sup> Experiments reported here have built upon previous work, but have addressed some unresolved issues identified previously and have demonstrated both the safety and efficacy of the NS-TLR7a/checkpoint inhibitor combination therapy.

In this study, the NS-TLR7a was shown to be stationary after injection and thus escaped rapid splenic clearance. Compared to systemic injection, the direct injection increases the ratio in the tumor to liver by >2500×. Although NS-TLR7a was retained at the local injection site, it had the ability to induce a robust systemic tumor antigen-specific immune response in the CT26 murine colon cancer model. The NS-TLR7a increased CD3<sup>+</sup> tumor infiltrating lymphocytes (TIL) by 4× and upregulated the expression level of the interferon  $\gamma$  (IFN- $\gamma$ ) gene compared to simply administering free TLR7a. Compared to unconjugated TLR7a, NS-TLR7a increased cytokine induction in sera that returned to baseline after 24 h. Toxicology studies of repeated doses further indicated that the NS-TLR7a had limited toxicity, and did not significantly affect the complete blood cell (CBC) count or hepatic function compared to the control vehicle. NS-TLR7a was, therefore, combined with a-PD-1 and a-CTLA-4 antibody therapies to better inhibit tumor growth by increasing the number of infiltrating immune cells 10–100× compared to the vehicle group in the CT26 tumor model. The CT26 tumor model had only a modest response to checkpoint inhibitor monotherapy. The triple combination therapy including NS-TLR7a, a-PD-1, and a-CTLA-4 induced both injected and contralateral tumors into full remission and improved survival rates from 0% with a-PD-1 and a-CTLA-4 monotherapy to 60% with NS-TLR7a plus a-PD-1 and

a-CTLA-4. Therefore, NS-TLR7a has potential to be an enhancer for current immunotherapy and may improve the outcome of cancer treatment in MMRp colon cancers and perhaps in other MMRp cancers.

Although small molecule TLR7 agonists are effective innate immune stimulators, there are two major problems for their clinical use: (1) because TLR7 is located in an endosomal compartment, effective endosomal delivery is required, and (2) TLR7a is quickly cleared after local administration. Our previous report demonstrated TLR7a conjugated to silica particles are quickly taken up by DCs and exhibit improved immune-potency.<sup>[16]</sup> In the present study, the biodistribution of the locally versus systemically administered NS-TLR7a was performed to investigate whether the conjugation of TLR7a onto nanoparticles improves sustained localization of the adjuvant at a local tumor injection site. NS-TLR7a was labeled with radioactive In<sup>111</sup> and injected intratumorally (i.t.) or intravenously (i.v.) into mice. Each mouse had two subcutaneous CT26 tumors in the right and left flanks but only one tumor was injected with radiolabeled NS-TLR7a. Planar  $\gamma$ -scintigraphy was used to monitor the particle distribution over 72 h (Figure 1a). Subsequently, organ biodistribution was performed by sacrificing the mice and measuring organ radioactivity 72-h postinjection (Figure 1b). Scintigraphy shown in Figure 1a demonstrates that systemically injected (i.v.) NS-TLR7a accumulated in the reticuloendothelial system organs, such as liver and spleen, which is typical of most i.v. injected nanoparticles immediately after injection.<sup>[24-26]</sup> This accretion continued with time (Figure 1a). Conversely, i.t. injected nanoparticles were retained at the injected tumor (right flank tumor) site for over 72 h, and only a small fraction of nanoparticles accumulated in the spleen, liver, or kidney. A small amount of i.t. injected nanoparticles traveled to the contralateral tumor (left flank tumor), as early as 24 h after i.t. injection (Figure 1a).

At 72-h postinjection, organs were harvested for gamma counting to quantify the nanoparticles in each organ (Figure 1b), for the systemically injected group, the nanoparticles mainly accumulated in liver (21.4%) and spleen (4.5%). A small portion of nanoparticles (0.3–0.4%) traveled to the tumor sites, which is likely due to a modest enhanced permeability and retention effect (EPR effect). Conversely, locally injected nanoparticles were mainly retained at the injected tumor (52.4%), and only small amounts of nanoparticles accumulated in the liver (1.4%) or spleen (0.5%). Compared to systemic injection, the direct injection increases the amount in the tumor 175× and decreases the amount in the liver 15× so the ratio in the tumor to liver increases by >2500×. A small amount of locally injected nanoparticles traveled to the distant tumor (0.3%). The lengthened retention time with the locally injected drug is consistent with the high efficacy (vide infra) of the i.t. injected agent. Such retention may further amplify the immune response induced by TLR7 activation because the drug can continuously stimulate and drive DCs to maturation. The lower amount of nanoparticle uptake at liver and spleen after direct tumor injection is consistent with NS-TLR7a residing in the tumor for a long period of time thereby having the potential to better activate the innate immune system and enhance tumor antigen presentation.

The effects of i.t. injected TLR7a with or without conjugation onto silica NS were tested in a CT26 mouse tumor model. Mice were implanted with 10<sup>6</sup> CT26 cells, and the treatment

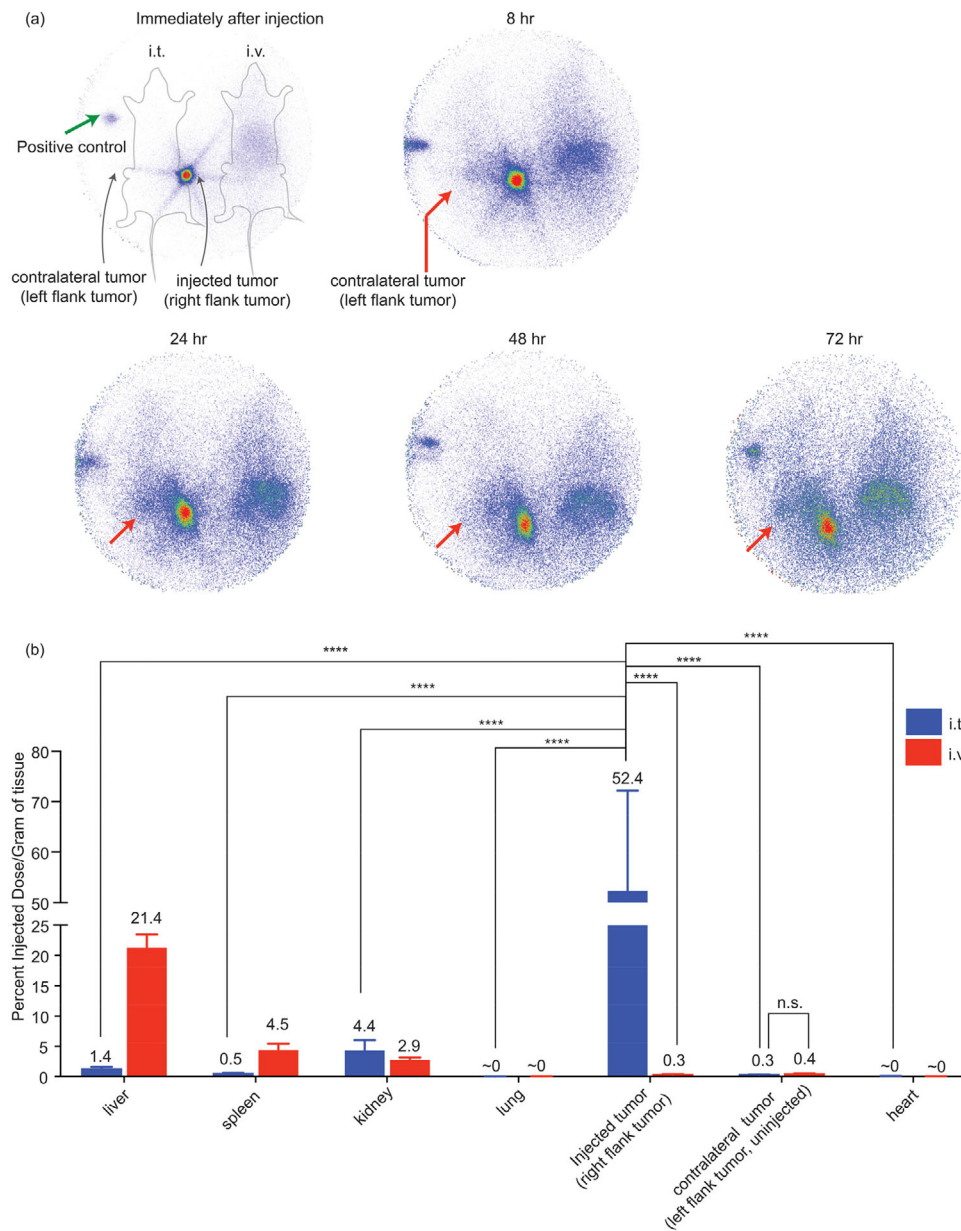


**Figure 1.** Locally injected NS-TLR7a retained at tumor and enhanced the immune response. a, b) Biodistribution of NS-TLR7a. In<sup>111</sup> labeled NS-TLR7a were i.t. and i.v. injected into CT26 tumor bearing mice ( $n = 5$  per group). Each mouse had two tumors in the right and left flanks to observe the particle distribution. a) Scintigraphy images of NS-TLR7a i.t. and i.v. injected mice. Pure In<sup>111</sup> was placed in a tube at the scintigraphic plane as a positive control (green arrow). The Red arrows pointing to the left flank tumor that was not injected with nanoparticles. b) i.t. (blue) and i.v. (red) injected mice were sacrificed and each organ was harvested for gamma counting at 72 h after NS-TLR7a injection. Numbers above bars indicate mean values, and  $\approx 0$  when the value is smaller than 0.1. Note that the gamma counts were divided by grams of tissue so the sum is not 100%. Data shown are means  $\pm$  standard error of the mean (SEM) of five mice in the representative of two independent experiments showing similar results. Data were analyzed with two-way ANOVA using Bonferroni post hoc test. c–h) Tumor growth regression in mice treated with i.t. NS-TLR7a monotherapy or controls. BALB/c mice were implanted with CT26 cells and treatment began when tumors reached 100 mm<sup>3</sup>. Mice ( $n = 5$  per group) were randomized and treated i.t. every other day with vehicle (PBS), silica NS, unconjugated TLR7a, or NS-TLR7a. Tumor tissues were collected on day 8 post-treatment for analysis. c) Experimental protocol. d) Average tumor growth curves. e, f) Immunohistochemistry (IHC) images of CD3<sup>+</sup> cells infiltrating into the tumor environments for (e) unconjugated TLR7a or (f) NS-TLR7a locally injected tumor. Representative IHC images are shown. g) Quantified CD3<sup>+</sup> T cells from 30 to 46 random IHC images per group. h) IFN- $\gamma$  gene expression level in tumor samples for vehicle, NS, TLR7a, and NS-TLR7a treated groups ( $n = 4$ –5 per group). Data shown are mean  $\pm$  SEM of the representative of two independent experiments showing similar results. One-way ANOVA with Bonferroni post hoc test was used for statistical significance analysis indicated as \*  $p < 0.05$ , \*\*  $p < 0.01$ , \*\*\*  $p < 0.001$ , and n.s. indicates not significant.

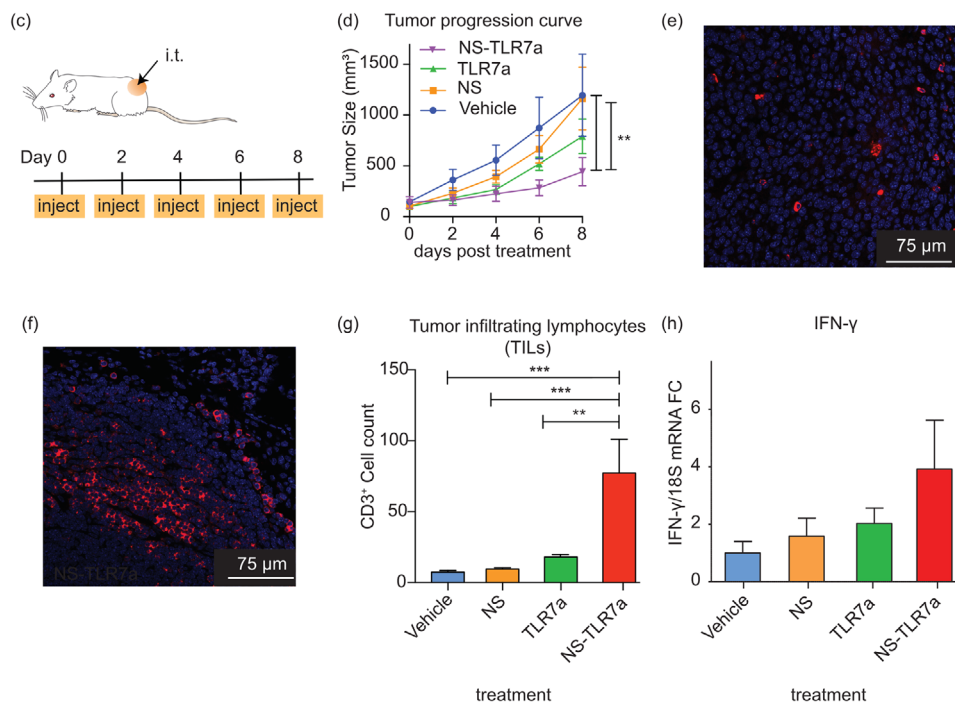


**Figure 1.** Continued

began when tumors reached 100 mm<sup>3</sup>. Tumor-bearing mice were i.t. treated with TLR7a (12.5 nmol per injection), NS-TLR7a (12.5 nmol TLR7a; 0.44 mg NS per injection), NS (0.44 mg per injection), or PBS every other day up to 8 days (Figure 1c). As shown in Figure 1d, the group treated with NS-TLR7a exhibited a significant tumor growth regression (>2×) compared to the vehicle or NS-treated group until 8 days after treatment.

Tumors were harvested on day 8 for immunohistochemical analysis, and CD3<sup>+</sup> cells were assessed for T cell subpopulations in the tumor microenvironment [note: CD3<sup>+</sup> cells include both cytotoxic T cells (CD8<sup>+</sup>) and T helper cells (CD4<sup>+</sup>)]. As shown in the representative immunohistochemistry images (Figure 1e,f), and the quantified data (Figure 1g), TLR7a conjugated onto NS showed a higher CD3<sup>+</sup> cell infiltration (>4×) compared to unconjugated TLR7a, which is likely due to prolonged retention of NS-TLR7a in the tumor environment relative to unconjugated ligand. This allows sufficient interaction time to activate DC and subsequent adaptive immunity. The control of bare NS injection did not lead to higher CD3<sup>+</sup> cell infiltration. Consistently, the tumors injected with NS-TLR7a exhibited higher IFN-γ expression (a critical cytokine for developing adaptive immunity against cancer cells) compared to vehicle, NS, or unconjugated TLR7a in harvested tumors (Figure 1h), which suggests the presence of activated TIL. These data are consistent with the concept that conjugating an immunotherapy agent onto NS can improve the in vivo therapeutic effect and modulate the immune cell response to a cancerous tumor.

The safety of NS-TLR7a was investigated. First, a systemic cytokine release study was performed to determine the potential toxic effects of the NS-TLR7a agent (Figure 2a–e). Single doses of either TLR7a (50 nmol per mouse), NS-TLR7a (50 nmol TLR7a; 1.76 mg NS), NS (1.76 mg per mouse), or vehicle were

administered i.t. and blood was collected at 0, 2, and 24 h postinjection. As shown in Figure 2b–e, there was a statistically significant increase of IL-6, IL-12, IP-10, and MCP-1 in blood samples collected from NS-TLR7a 2 h postinjection ( $p < 0.005$ ) for IL-6, IL-12, IP-10, and MCP-1, respectively. IL-6 and IL-12 are downstream cytokines of TLR7 signaling and can help differentiate T cells.<sup>[27,28]</sup> IP-10 and MCP-1 are chemokines that can regulate the migration of immune cells.<sup>[29]</sup> After 24 h, all treated samples returned to baseline levels. No weight loss or behavioral changes were observed in any treatment groups at the given doses. These data show that NS-TLR7a induced only a transient systemic cytokine response which returns to basal levels by 24 h.

Systemic toxicology was also evaluated for repeatedly dosed NS-TLR7a because an effective immunostimulatory agent (i.e., TLR7 agonists) may result in undesired immune-related adverse effects. Four to five female BALB/c mice bearing CT26 tumors on right and left flanks were i.t. injected with 12.5 nmol of NS-TLR7a or vehicle (PBS) every other day for six treatments, and body weight and behavior were observed over the time of treatment (Figure 2f). Repeated treatments of NS-TLR7a or vehicle did not induce body weight loss or behavioral changes (reduced activity, piloerection, lethargy, or tachypnea). On day 14, blood and sera were collected for hematological and biochemical analysis (Figure 2g,h and Figure S1, Supporting Information). At the given dose and administration routes, NS-TLR7a did not induce hepatic, pancreatic, or renal dysfunctions (Figure S1, Supporting Information). The electrolyte composition also remained stable after treatment. A minor adverse event in the studies was a modest erythrocytopenia (Figure 2g) that has been previously reported in an oral dosing study of a TLR7a.<sup>[30]</sup> This effect attenuated throughout the study.<sup>[30]</sup> Although it was not statistically significant, local NS-TLR7a treatment induced a net reduction

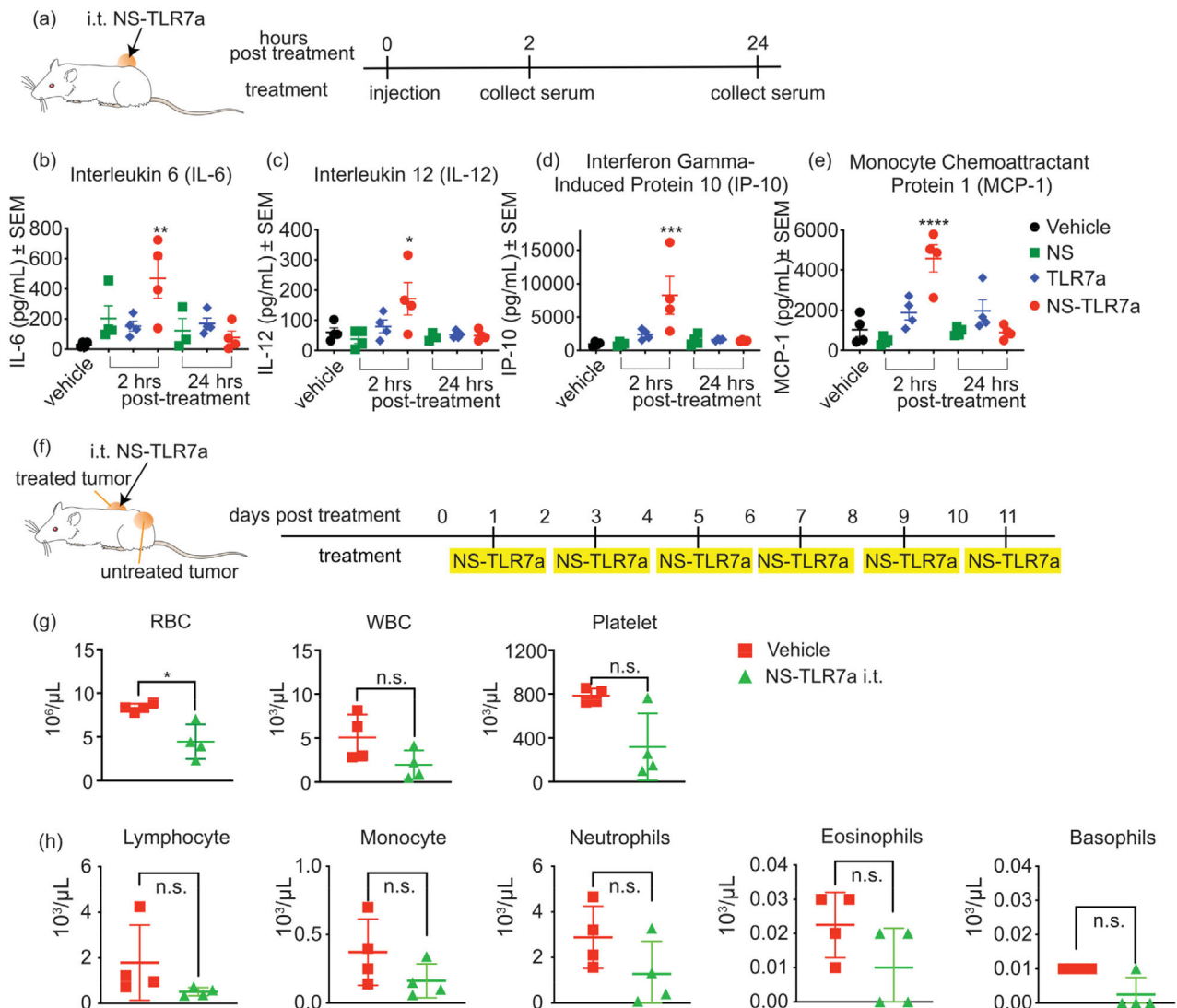


**Figure 2.** Negligible systemic toxicity by i.t. injection of NS-TLR7a. a) Single doses of TLR7a (50 nmol per mouse), NS-TLR7a (50 nmol TLR7a; 1.8 mg NS), NS (1.8 mg/mouse), or vehicle were i.t. administered ( $n = 4$  per group). Blood was collected at 0, 2, and 24 h and sera were isolated. Cytokine levels for of b) IL-6, c) IL-12, d) IP-10, and e) MCP-1 were measured using Luminex beads assays. Each dot indicates an individual animal and horizontal and vertical bars are means  $\pm$  SEM. One-way ANOVA compared to vehicle group with Bonferroni post hoc test was used for assessing statistical significance. f-h) Toxicology investigation of NS-TLR7a. f) Female BALB/c mice ( $n = 4$ –5 per group) each bearing two tumors on the right and left flanks were i.t. injected with NS-TLR7a or vehicle every other day for a total of six doses. Whole blood and sera were collected on day 14 post-treatment for complete blood count and biochemistry analyses. The investigation includes: g) red blood cells, white blood cells, and platelets. h) leukocyte subset. n.s. indicates not significant and analysis indicated as \* ( $p < 0.05$ ), \*\* ( $p < 0.01$ ), \*\*\* ( $p < 0.001$ ), and \*\*\*\* ( $p < 0.0001$ ).

of the white blood cells in circulation, including lymphocytes, monocytes, neutrophils, eosinophils, and basophils (Figure 2h). In Figure S2 (Supporting Information), the cell numbers of each subtype of white blood cell (neutrophils, eosinophils, basophils, lymphocytes, and monocytes) were combined and averaged. The average number was normalized to the average number of vehicle treated animals. Figure 2h and Figure S2 (Supporting Information) indicated that repeated NS-TLR7a therapy had a noticeable trend of reduction after NS-TLR7a therapy compared to the vehicle group ( $p = 0.0523$  in Figure S2, Supporting Information). These data are consistent with other reports that low molecular weight TLR7a induce reversible lymphopenia which

is type I IFN-dependent and an on-target adverse effect of this therapy.<sup>[31,32]</sup> Since lymphopenia induced by TLR7a therapy is transient,<sup>[33,34]</sup> CBC was performed 24 h post-subcutaneous (s.c.) s.c. injection (Table S1, Supporting Information). Neither NS-TLR7a nor TLR7a treatment showed different counts of white blood cells or red blood cells compared to vehicle group, which shows that local injection of NS-TLR7a and TLR7a had negligible adverse effects on mice. Collectively, a repeated local injection, but not a local single injection of NS-TLR7a, has potential to induce erythrocytopenia and lymphopenia, which suggests that further optimization of the dosing schedule will be necessary.

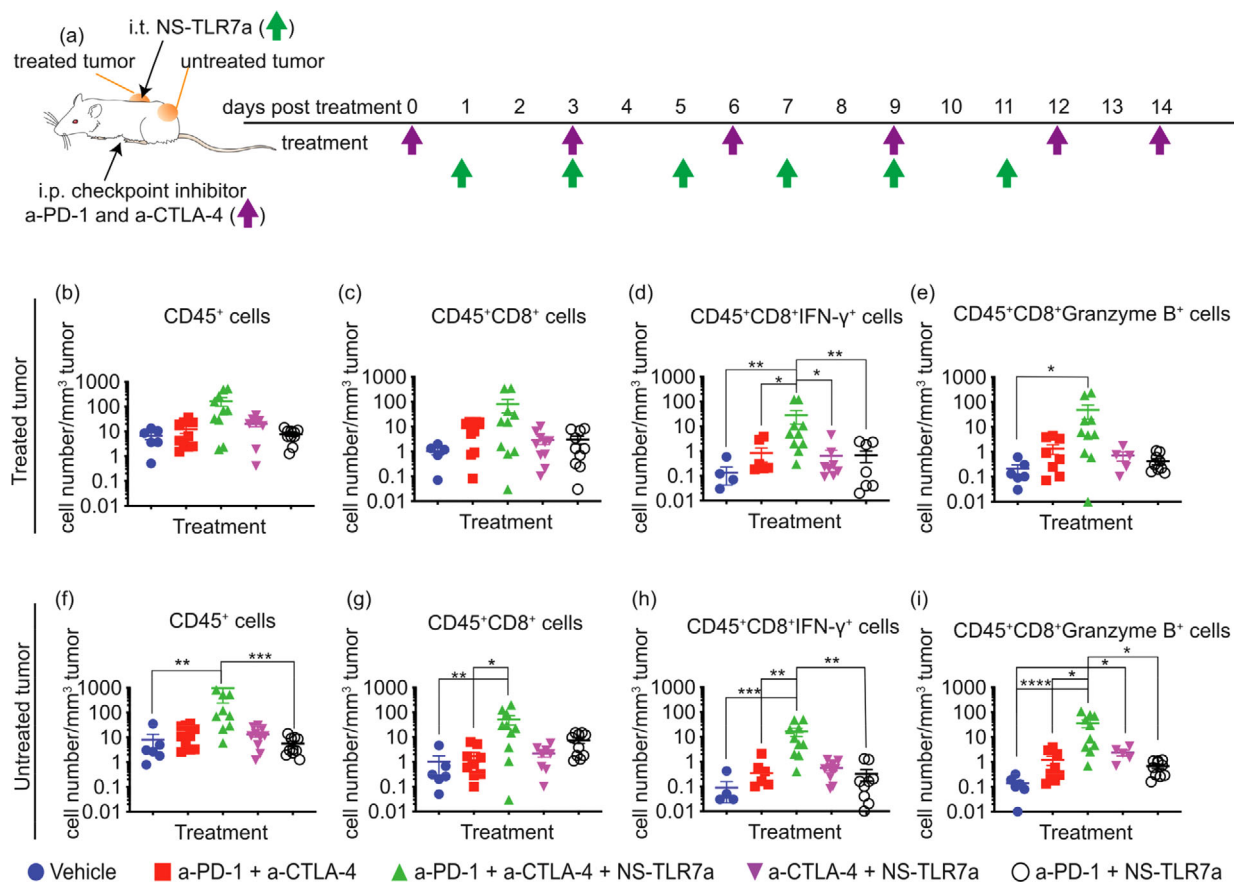


**Figure 3.** TIL analysis and tumor progression curve following the combination therapy. a–i) TIL analysis of NS-TLR7a combination therapy. CT26 colon tumor cells were s.c. implanted into female BALB/c mice (4–5 mice per group) at right and left flanks. NS-TLR7a, a-PD-1, and a-CTLA-4 were combined to treat CT26 tumor-bearing mice and the immune cell populations in the tumor microenvironment were investigated. a) Experimental protocol. Day 0 is defined as the day of the first treatment; NS-TLR7a was i.t. injected into one flank tumor (treated tumor) and checkpoint inhibitors were i.p. injected. In the treated tumor, b) CD45<sup>+</sup>, c) CD45<sup>+</sup>CD8<sup>+</sup>, d) CD45<sup>+</sup>CD8<sup>+</sup>IFN- $\gamma$ <sup>+</sup>, and e) CD45<sup>+</sup>CD8<sup>+</sup>granzyme B<sup>+</sup> cells were enumerated. The same analyses were done on the untreated contralateral flank tumors (f)–(i). Immune cell populations in treated and untreated tumors were compared. Each dot indicates an individual animal and vertical and horizontal bars are means  $\pm$  SEM of two independent pooled experiments showing similar results. Data were analyzed by the Kruskal–Wallis test using Dunn’s multiple comparisons *post hoc* test. j–p) Suppression of tumor growth and survival rates with combination therapy. CT26 colon tumor-bearing mice (8–10 mice per group) were treated with vehicle, combined checkpoint inhibitors (a-PD-1+a-CTLA-4), and checkpoint inhibitors combined with NS-TLR7a (a-PD-1+a-CTLA-4+NS-TLR7a). The progressions of both (j)–(l) treated tumors and (m)–(o) untreated tumors were monitored. The treatment protocol is shown in (a). Checkpoint inhibitors (100  $\mu$ g; a-PD-1 and a-CTLA-4) were injected i.p. three times per week. A 12.5 nmol NS-TLR7a was i.t. injected every other day. Mice were sacrificed when tumors reached 2000 mm<sup>3</sup> or ulceration occurred as required by the UCSD IACUC guideline (policy 9.04). Data were pooled from two independent experiments, which showed similar results. p) Survival was monitored until day 90 and a Logrank test was used for significance. \*means  $p < 0.05$ , \*\*means  $p < 0.01$ , \*\*\*means  $p < 0.001$ , and \*\*\*\*means  $p < 0.0001$ .

TLR agonists, being strong immunostimulatory agents, can reverse the immunosuppressive microenvironment created by tumors.<sup>[35,36]</sup> Intratumoral treatment with TLR7a increases the ratio of M1 (antitumor phenotype) to M2 (protumor phenotype) tumor associated macrophages.<sup>[36]</sup> TLR7a also causes rapid reduction of myeloid-derived suppressor cells (MDSC) within the tumor microenvironment.<sup>[37]</sup> The combined TLR7a and PD-L1 blockade results in a reduced number of T regulatory cells in the tumor microenvironment.<sup>[38]</sup> The above data (Figures 1 and 2) showed that NS-TLR7a therapy was safe and reduced tumor progression; however, monotherapy with NS-TLR7a only resulted in partial tumor remission. Given the known efficacy of anti-PD-1 (a-PD-1) and anti-CTLA4 (a-CTLA-4) therapies and their ligand expression in this murine tumor type as well as human

colorectal cancer,<sup>[39]</sup> a-PD-1 and a-CTLA-4 therapies were combined with NS-TLR7a therapy. As single agents, both a-PD-1 and a-CTLA-4 are known to have modest therapeutic effects; therefore, the potential treatment combinations were first screened by determining the TIL population. Five treatment groups were used to study the cell population upon combination therapy: (1) vehicle, (2) a-PD-1+a-CTLA-4, (3) NS-TLR7a + a-CTLA-4 + a-PD-1 (triple therapy), (4) NS-TLR7a + a-PD-1, and (5) NS-TLR7a + a-CTLA-4. Single agent therapy was not chosen as a group because previous studies showed that single blockade of a checkpoint pathway has limited efficacy on CT26 tumors.<sup>[40]</sup> The treatment protocol is shown in Figure 3a: NS-TLR7a was i.t. injected and checkpoint inhibitors a-PD-1 and/or a-CTLA-4 were injected via intraperitoneal (i.p.) routes. Both the directly injected tumors

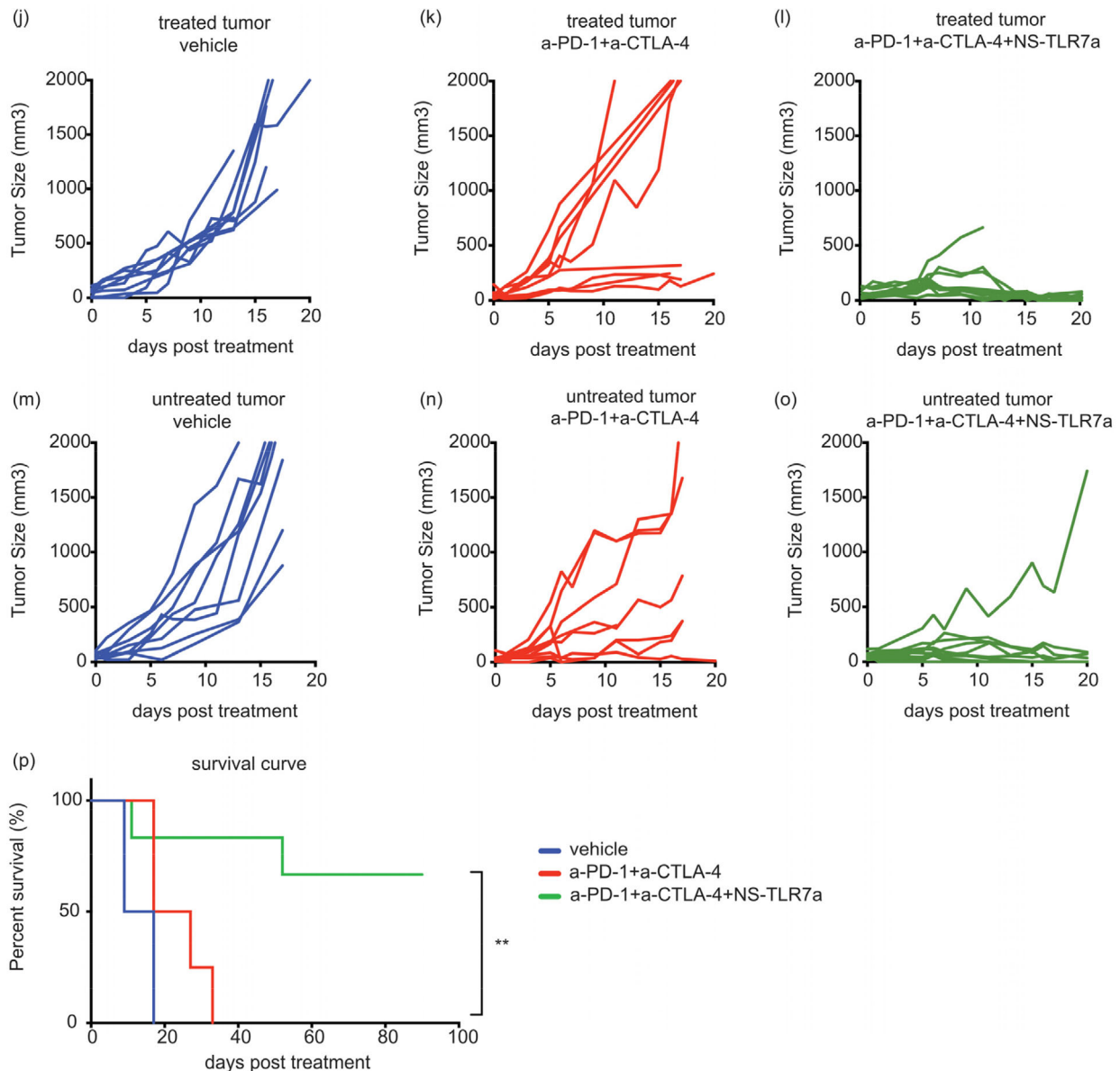


**Figure 3.** Continued

(treated tumor) and the contralateral not directly injected tumors (untreated tumors) were harvested on day 14 after the first treatment to study the TIL in the tumor environment. The NS-TLR7a+a-PD-1+a-CTLA-4 (triple therapy) treated group showed a greater infiltrated number of CD45<sup>+</sup> (leukocytes) and CD8<sup>+</sup> cells (cytotoxic T cells) in both treated and untreated tumors (Figure 3b,c,f, and g) compared to the other therapy combinations. About a 100-fold increase in CD45<sup>+</sup>CD8<sup>+</sup> cells ( $p = 0.0991$  and  $0.0094$ ), in CD45<sup>+</sup>CD8<sup>+</sup>IFN- $\gamma$ <sup>+</sup> cells ( $p = 0.0083$  and  $0.005$ ), and in CD45<sup>+</sup>CD8<sup>+</sup>granzyme B<sup>+</sup> cells ( $p = 0.0132$  and  $<0.0001$ ) was observed in both treated and contralateral tumors, respectively, following triple therapy. This shows that the TIL were activated (Figure 3d,e,h,i). The CD8<sup>+</sup>IFN- $\gamma$ <sup>+</sup> cells indicate activation of cytotoxic T cells to destroy tumor cells and the CD8<sup>+</sup> granzyme B<sup>+</sup> cells can mediate apoptosis.<sup>[41-43]</sup> The increase of immune cells,

IFN- $\gamma$ <sup>+</sup> and granzyme B<sup>+</sup> cells, in both treated and contralateral tumors demonstrate that the improvement of the immune response for the triple therapy is systemic, since only one flank tumor site was injected with NS-TLR7a.

After determining that triple therapy with NS-TLR7a, a-PD-1, and a-CTLA-4 showed the highest number of activated lymphocyte infiltration, the efficacy of triple therapy to suppress tumor growth and promote long-term survival was investigated in the CT26 model. The combined checkpoint inhibitors (a-PD-1+a-CTLA-4) were reported to have promising therapeutic treatment outcome,<sup>[4]</sup> and, therefore, this was chosen for comparison with triple therapy which consisted of NS-TLR7a, a-PD-1, and a-CTLA-4. To assess abscopal effects by induction of systemic anti-tumor immune responses, only one (right side) of the two flank tumors was injected with NS-TLR7a; the treatment protocol is

shown in Figure 3a. As shown in Figure 3j–p, the triple therapy with NS-TLR7a, a-PD-1, and a-CTLA-4 induced complete remission at the treated right side tumor (complete remission rate: 80%) as well as at the contralateral untreated tumor (complete remission rate: 60%). To the authors' knowledge, this is the highest reported systemic remission rate for any two tumor murine colon cancer model in which the starting tumor size is 100 mm<sup>3</sup> that use nanoparticle-based TLR7/8 agonists combined with checkpoint inhibitors.

A mechanism of combination therapy is proposed in Scheme S2 (Supporting Information). This work shows NS-TLR7a is retained at the tumor after injection and activates immune cells. T lymphocytes also infiltrate into the tumors. The a-PD-1 and a-CTLA-4 antibodies are known to block inhibitory pathways and restore cytotoxic activity of T cells. Several previous studies have used nanoparticle-based TLR7/8 agonists combined with checkpoint inhibitors or chemodrugs to treat cancer, as summarized in Table S2 (Supporting Information). Combination therapy using polymer nanoparticles such as PLGA/PEG to deliver agonists demonstrated a delay in tumor growth<sup>[23,44]</sup>; however, most studies employed a single-tumor-bearing model, and therefore, it is unknown if these treatments induced abscopal effect that triggers systemic antigen-specific responses with the potential to treat metastatic tumors. Agonists loaded on cyclodextrin combined with a-PD-1 showed excellent therapeutic outcome on a two-tumor mouse model<sup>[19]</sup>; however, the study used the MC38 tumor model, which is intrinsically responsive to PD-1/PD-L1 blockade.<sup>[14]</sup>

The earlier nanoparticle biodistribution study showed that locally injected nanoparticles mainly stay at the injected site (Figure 1). This observation suggests that the tumor inhibition effects observed for the contralateral tumor is due to a systemic adaptive immune response and less likely due to the small amount of NS-TLR7a that traveled to the distant tumor. To further validate that triple therapy induced tumor-specific adaptive immune responses, the mice with tumor remission after triple therapy were implanted with CT26 cells on a nontreated flank site, and the growth of rechallenged tumors monitored. No tumor growth was detected in the challenged mice (rechallenged mouse tumor free rate: 100%), proving that immune memory was produced during the initial treatment/remission.

In this study, the therapeutic efficacy of TLR7a conjugated to silica NS was described when used as monotherapy and as combination therapy with checkpoint inhibitors. Conjugating TLR7a onto NS lengthened the TLR7a retention at the locally injected tumor. As shown in the biodistribution study, i.t injected NS-TLR7a was retained 175× higher in the tumor and 15× lower in the liver when compared to i.v. injected NS-TLR7a. When i.t. NS-TLR7a was combined with checkpoint inhibitor therapy to treat a colorectal cancer model (CT26) that only has modest responses to checkpoint inhibitor immunotherapy, a 10–100× increase in tumor infiltrating lymphocytes and complete tumor remission was observed; treated and contralateral (untreated) tumors had complete remission rates of 80% and 60%, respectively. Triple therapy induced abscopal effects on distant tumors, and the cured treated mice that were rechallenged with CT26 cells rejected the implanted cells, indicating that the triple therapy induced tumor antigen-specific systemic immune response. In summary, i.t. injection of NS conjugated TLR7a may provide a method to induce

a safe and more robust antitumor immune response to checkpoint inhibitor immunotherapy, against cancer types that are less responsive to checkpoint inhibitor treatments.

## Experimental Section

**Materials:** Diethylenetriamine (DETA, Cat. No. D93856), Tetramethyl orthosilicate (TMOS), trimethoxy(phenyl)silane (TMPS), *N*-hydroxysuccinimide (NHS, Cat. No. 130 672), *N*-(3-dimethylaminopropyl)-*N'*-ethylcarbodiimide (EDC), and organic solvents were purchased from Sigma Aldrich (St. Louis, MO). Hundred nanometer polystyrene templates were purchased from Polysciences Inc. (Warrington, PA). 2-(4-Isothiocyantobenzyl)-diethylenetriaminepentaacetic acid (DTPA) was purchased from Macrocyclics (Dallas, TX). <sup>111</sup>InCl<sub>3</sub> was purchased from Covidien (Mansfield, MA). 4-[6-Amino-2-(2-methoxyethoxy)-8-oxo-7H-purin-9(8H-yl)methyl]benzoic acid (1V209) was synthesized as previously described.<sup>[45]</sup> Anti-mouse PD-1 (CD279) antibodies (clone RMP1-14, Cat. No. BP0146) or anti-mouse CTLA-4 (CD152) antibodies (clone 9D9, Cat. No. BP0164) were purchased from BioXcell (West Lebanon, NH). Roswell Park Memorial Institute (RPMI) medium 1640 (Cat. No. 11875-093, Gibco) and Dulbecco's Modified Eagle's Medium (DMEM, Cat. No. 15-013-CV, Corning) were supplemented with 10% fetal bovine serum (Cat. No. 35-011-CV, Corning) and 100 U mL<sup>-1</sup> penicillin, 100 µg mL<sup>-1</sup> streptomycin, 292 µg mL<sup>-1</sup> glutamine (Cat. No. 10378-016, Thermo Fisher Scientific) to prepare complete media (RPMI-10 or DMEM-10).

**Animals and Tumor Model:** Mouse colon cancer cell line CT26 (Cat. No. CRL-2638) was purchased from American Type Culture Collection (ATCC). Six to eight week old female BALB/c mice were purchased from The Jackson Laboratory. 10<sup>6</sup> cells 50 µL<sup>-1</sup> in PBS were s.c. injected into the right and left flanks, and treatment was started at a tumor size of approximately 100 mm<sup>3</sup>. Tumor volume was determined by caliper with the modified ellipsoidal formula: volume (mm<sup>3</sup>) = (width × width × length)/2.<sup>[46]</sup> Pain and distress in tumor-bearing mice were closely monitored. Procedures causing more than momentary or slight pain or distress must be performed with appropriate anesthesia. If a tumor becomes ulcerated or necrotic, or if a single subcutaneous tumor exceeds 2 cm in diameter, immediate euthanasia is performed. For multiple subcutaneous tumors, when the combined volume of tumors exceeds 4 cm<sup>3</sup>, euthanasia is performed. All procedures and protocols were approved by the UC San Diego Institutional Animal Care and Use Committee (IACUC).

**Histological Analysis:** Tissue samples were fixed in 10% formalin (one part of stock formaldehyde (37–40%) and nine parts of water) and transferred to 70% ethanol before paraffin block processing and sectioning. Immunohistochemistry used rat anti-CD3 antibody (1:200, Cat. No. ab11089, Abcam). Images were obtained using a 10× dry objective on a SP8 Leica confocal microscope. A minimum of eight fields were examined per section and at least three sections per sample. Cell count analysis was performed using ImageJ and Leica proprietary software.

**RNA Extraction and RT-qPCR Expression Analysis:** CT26-derived tumor tissues from the *in vivo* studies were collected and flash frozen to –80 °C for storage. Tissue lysates were prepared with a Next Advance NA-01 tissue homogenizer, in isolation buffer (sucrose (MW 342.3) 70 × 10<sup>-3</sup> m; mannitol (MW 182.2) 190 × 10<sup>-3</sup> m; HEPES pH 7–8, 20 × 10<sup>-3</sup> m; EDTA pH 8, 0.2 × 10<sup>-3</sup> m) supplemented with protease and phosphatase inhibitors (1:100 dilution; Cat. No. 535 140, P5726, Sigma-Aldrich) and RNASE-free homogenization beads (Cat. No. SSB14B and SSB32, Next-Advance). Total RNA was extracted from cells and/or tissues lysates using the Quick-RNA Miniprep Kit (Cat. No. 11-328, Zymo Research), according to manufacturer's instructions, and reverse transcribed using the iScript cDNA Synthesis Kit (Cat. No. 170–8891, Bio-Rad). qPCR was done using SYBR Green and results were analyzed using the ΔΔCq method<sup>[47]</sup> and normalized to housekeeping genes 18S and GAPDH. Primer sequences were designed using NCBI's Primer BLAST and spanned exon-exon junctions. A list of primer sequences used is presented in Table S2 (Supporting Information).

**Biodistribution:** NS-TLR7a was prepared as previously described.<sup>[16]</sup> One milliliter of 3 mg mL<sup>-1</sup> of NS-TLR7a was functionalized with 2 μL of 1 mg mL<sup>-1</sup> DTPA and pulse-vortexed for 24 h. Functionalized NS-TLR7a was washed and resuspended in 0.1 M citrate buffer (pH 6) to 2 mg mL<sup>-1</sup> solution. Two milligrams of the NS were incubated with ≈100 μCi of In<sup>111</sup> chloride for 30 min. Radiolabeled NS-TLR7a was washed twice with buffer and twice with MilliQ purified water. During the wash procedure, the In<sup>111</sup>-labeled NS and the supernatant were measured by dose calibrator to track the In<sup>111</sup> retention. After washing, In<sup>111</sup>-NS-TLR7a was resuspended to 4 mg mL<sup>-1</sup> in MilliQ purified water for in vivo injection. 100 μL of In<sup>111</sup>-NS-TLR7a was injected into two-tumor-bearing mice i.v. or i.t. Mice were imaged via planar scintigraphy immediately, and then 8, 24, 48, and 72 h postinjection. After 72 h, mice were sacrificed. Spleen, lung, heart, right tumor (treated), left tumor (untreated), kidney, and liver were collected and the gamma intensity counted.

**Toxicology Analysis:** (1) Sera Cytokine Analysis: Female BALB/c bearing one CT26 tumor was i.t. injected with single doses of TLR7a (50 nmol per mouse), NS-TLR7a (50 nmol TLR7a; 1.8 mg NS), NS (1.8 mg per mouse), or vehicle ( $n = 4$  per group). Blood samples were collected at 0, 2, and 24 h after treatment, and sera were isolated. Luminex bead assays were used to determine the systemic cytokine levels of IL-6, IL-12, IP-10, and MCP-1, and were measured with the use of a MAGPIX machine (Luminex Corporation). (2) Repeated dose toxicology assessment: Female BALB/c mice ( $n = 4-5$  per group), each bearing two CT26 tumors on the right and left flanks, were i.t. injected with NS-TLR7a or vehicle every other day for a total of 6 doses. Whole blood and sera were collected on day 14 post-treatment for CBC and biochemistry analysis. For CBC analysis, ≈50 μL of whole blood was collected in BD microtainer ethylenediaminetetraacetic acid (EDTA) tubes (Cat. No. 365 974, BD Vacutainer Labware Medical). The tubes were flicked immediately after filling and inverted several times to distribute the anticoagulant. For biochemistry analysis, the test requires a minimum of 120 μL of sera in lithium heparin tubes (Cat. No. 22 040 104, Fisher Scientific). Both CBC and biochemistry analyses were performed by UCSD Murine Hematology and Coagulation Core Laboratory. (3) Single dose toxicology assessment: Four to five BALB/c mice per group were s.c. injected with one dose of TLR7a (12.5 nmol per injection), NS-TLR7a (12.5 nmol TLR7a; 0.44 mg silica nanoshells per injection), silica NS (0.44 mg per injection), or PBS. Approximately 50 μL of whole blood were collected in the BD microtainer EDTA tubes. The tubes were flicked immediately after filling and inverted several times to distribute the anticoagulant. CBC analysis was performed by UCSD Murine Hematology and Coagulation Core Laboratory.

**Analysis of Tumor-Infiltrating Immune Cells:** Each mouse had two CT26 tumors on the right and left flanks. Hundred micrograms of checkpoint inhibitor, a-PD-1 and/or a-CTLA-4 antibodies were injected i.p. three times weekly (day 0, 3, 6, 9, 12, 14). A 12.5 nmol of NS-TLR7a in 50 μL PBS were injected i.t. every other day for a total of six doses (day 1, 3, 5, 7, 9, 11). Day 0 was defined as the day of first treatment. Mice were sacrificed on day 14 for tumor infiltrating lymphocyte analysis. Tumors were dissociated into cell suspension using a mouse tumor dissociation kit with use of the gentleMACS Octo Dissociator according to the manufacturer's protocol (Miltenyi Biotec). Cell suspensions were incubated and stained with cocktails of anti-mouse CD45 (Cat. No. 103 114, BioLegend) and anti-mouse CD8 (Cat. No. 48-0081, Invitrogen) antibodies at 4 °C for 30 min. Fixation/Permeabilization Solution kits were used for intracellular IFN-γ staining (Cat. No. 17-7311, BD Biosciences) and granzyme B (Cat. No. 515 403, BioLegend). The stained cells were analyzed by flow cytometry (MACS Quant, Miltenyi Biotec).

**Statistical Analysis:** The data were pooled from 2 to 4 rounds of experiments and presented as means with standard error of the mean (SEM). To determine the significance between the means of two groups, a t test with Welch's correction was performed. One-way ANOVA was used with a Bonferroni post hoc test to compare means of two or more samples. Statistical comparisons of continuous variables between groups was performed using two-way ANOVA followed by a Bonferroni post hoc test. For TIL data, a Kruskal–Wallis test was performed with Dunn's multiple comparisons test. n.s. indicates not significant and analyses are indicated as \* ( $p < 0.05$ ), \*\* ( $p < 0.01$ ), \*\*\* ( $p < 0.001$ ), and \*\*\*\* ( $p <$

0.0001). GraphPad Prism software 8.3.1 version was used for all statistical analyses.

## Supporting Information

Supporting Information is available from the Wiley Online Library or from the author.

## Conflict of Interest

This study was funded by the National Institutes of Health grants U54CA132379, 5T32CA153915, and ViewPoint Medical Inc. Sarah Blair's spouse is co-founder, CEO and has equity interest in ViewPoint Medical Inc. Andrew Kummel and William Troglar are scientific advisors and have an equity interest in ViewPoint Medical Inc. The terms of this arrangement have been reviewed and approved by the University of California, San Diego, in accordance with its conflict of interest policies.

## Keywords

combination therapy, nanoparticles-based immunotherapy, silica nanoshells, TLR7 agonists

Received: November 5, 2019

Revised: February 9, 2020

Published online: March 16, 2020

- [1] K. K. Ciombor, C. Wu, R. M. Goldberg, *Annu. Rev. Med.* **2015**, *66*, 83.
- [2] M. G. Fakih, *J. Clin. Oncol.* **2015**, *33*, 1809.
- [3] F. S. Hodi, J. Chesney, A. C. Pavlick, C. Robert, K. F. Grossmann, D. F. McDermott, G. P. Linette, N. Meyer, J. K. Giguere, S. S. Agarwala, M. Shaheen, M. S. Ernstoff, D. R. Minor, A. K. Salama, M. H. Taylor, P. A. Ott, C. Horak, P. Gagnier, J. Jiang, J. D. Wolchok, M. A. Postow, *Lancet Oncol.* **2016**, *17*, 1558.
- [4] J. Duraiswamy, K. M. Kaluza, G. J. Freeman, G. Coukos, *Cancer Res.* **2013**, *73*, 3591.
- [5] S. P. Arora, D. Mahalingam, *J. Gastrointest. Oncol.* **2018**, *9*, 170.
- [6] S. Emambux, G. Tachon, A. Junca, D. Tougeron, *Expert Opin. Biol. Ther.* **2018**, *18*, 561.
- [7] D. T. Le, J. N. Durham, K. N. Smith, H. Wang, B. R. Bartlett, L. K. Aulakh, S. Lu, H. Kemberling, C. Wilt, B. S. Luber, F. Wong, N. S. Azad, A. A. Rucki, D. Laheru, R. Donehower, A. Zaheer, G. A. Fisher, T. S. Crocenzi, J. J. Lee, T. F. Greden, A. G. Duffy, K. K. Ciombor, A. D. Eyring, B. H. Lam, A. Joe, S. P. Kang, M. Holdhoff, L. Danilova, L. Cope, C. Meyer, et al., *Science* **2017**, *357*, 409.
- [8] M. J. Overman, R. McDermott, J. L. Leach, S. Lonardi, H.-J. Lenz, M. A. Morse, J. Desai, A. Hill, M. Axelson, R. A. Moss, M. V. Goldberg, Z. A. Cao, J.-M. Ledeine, G. A. Maglinte, S. Kopetz, T. André, *Lancet Oncol.* **2015**, *18*, 1182.
- [9] D. T. Le, J. N. Uram, H. Wang, B. R. Bartlett, H. Kemberling, A. D. Eyring, A. D. Skora, B. S. Luber, N. S. Azad, D. Laheru, B. Biedrzycki, R. C. Donehower, A. Zaheer, G. A. Fisher, T. S. Crocenzi, J. J. Lee, S. M. Duffy, R. M. Goldberg, A. de la Chapelle, M. Koshiji, F. Bhaijee, T. Huebner, R. H. Hruban, L. D. Wood, N. Cuka, D. M. Pardoll, N. Papadopoulos, K. W. Kinzler, S. Zhou, T. C. Cornish, et al., *N. Engl. J. Med.* **2015**, *372*, 2509.
- [10] M. M. Boyiadzis, J. M. Kirkwood, J. L. Marshall, C. C. Pritchard, N. S. Azad, J. L. Gulley, *J. Immunother. Cancer* **2018**, *6*, 35.

- [11] D. T. Le, J. N. Uram, H. Wang, B. Bartlett, H. Kemberling, A. Eyring, N. S. Azad, D. Laheru, R. C. Donehower, T. S. Crocenzi, R. M. Goldberg, G. A. Fisher, J. J. Lee, T. F. Greten, M. Koshiji, S. P. Kang, R. A. Anders, J. R. Eshleman, B. Vogelstein, L. A. Diaz, *J. Clin. Oncol.* **2016**, *34*, 103.
- [12] C. Fellner, *Pharm. Ther.* **2017**, *42*, 262.
- [13] J. C. Castle, M. Loewer, S. Boegel, J. de Graaf, C. Bender, A. D. Tadmor, V. Boisguerin, T. Bukur, P. Sorn, C. Paret, M. Diken, S. Kreiter, Ö. Türeci, U. Sahin, *BMC Genomics* **2014**, *15*, 190.
- [14] M. Efremova, D. Rieder, V. Klepsch, P. Charoentong, F. Finotello, H. Hackl, N. Hermann-Kleiter, M. Löwer, G. Baier, A. Krogsdam, Z. Trajanoski, *Nat. Commun.* **2018**, *9*, 32.
- [15] G. Yu, Y. Wu, W. Wang, J. Xu, X. Lv, X. Cao, T. Wan, *Cell Mol. Immunol.* **2019**, *16*, 401.
- [16] C.-H. Huang, N. Mendez, O. H. Echeagaray, J. Weeks, J. Wang, C. N. Vallez, N. Gude, W. C. Trogler, D. A. Carson, T. Hayashi, A. C. Kummel, *ACS Appl. Mater. Interfaces* **2019**, *11*, 26637.
- [17] M. Tosolini, A. Kirilovsky, B. Mlecnik, T. Fredriksen, S. Mauger, G. Bindea, A. Berger, P. Bruneval, W.-H. Fridman, F. Pagès, J. Galon, *Cancer Res.* **2011**, *71*, 1263.
- [18] Q. Chen, L. Xu, C. Liang, C. Wang, R. Peng, Z. Liu, *Nat. Commun.* **2016**, *7*, 13193.
- [19] C. B. Rodell, S. P. Arlauckas, M. F. Cuccarese, C. S. Garris, R. Li, M. S. Ahmed, R. H. Kohler, M. J. Pittet, R. Weissleder, *Nat. Biomed. Eng.* **2018**, *2*, 578.
- [20] H. Kim, D. Sehgal, T. A. Kucaba, D. M. Ferguson, T. S. Griffith, J. Panyam, *Nanoscale* **2018**, *10*, 20851.
- [21] V. Alcazer, P. Bonaventura, L. Tonon, S. Wittmann, C. Caux, S. Depil, *Eur. J. Cancer* **2019**, *108*, 55.
- [22] L. Nuhn, S. De Koker, S. Van Lint, Z. Zhong, J. P. Catani, F. Combes, K. Deswarte, Y. Li, B. N. Lambrecht, S. Lienenklaus, N. N. Sanders, S. A. David, J. Tavernier, B. G. De Geest, *Adv. Mater.* **2018**, *30*, 1803397.
- [23] D. Schmid, C. G. Park, C. A. Hartl, N. Subedi, A. N. Cartwright, R. B. Puerto, Y. Zheng, J. Maiarana, G. J. Freeman, K. W. Wucherpfennig, D. J. Irvine, M. S. Goldberg, *Nat. Commun.* **2017**, *8*, 1747.
- [24] X. Duan, Y. Li, *Small* **2013**, *9*, 1521.
- [25] A. L. Brown, M. P. Kai, A. N. DuRoss, G. Sahay, C. Sun, *Nanomaterials* **2018**, *8*, 410.
- [26] L. Yang, H. Kuang, W. Zhang, Z. P. Aguilar, H. Wei, H. Xu, *Sci. Rep.* **2017**, *7*, 3303.
- [27] S. E. Macatonia, N. A. Hosken, M. Litton, P. Vieira, C. S. Hsieh, J. A. Culpepper, M. Wysocka, G. Trinchieri, K. M. Murphy, A. O'Garra, *J. Immunol.* **1995**, *154*, 5071.
- [28] T. Tanaka, M. Narazaki, T. Kishimoto, *Cold Spring Harbor Perspect. Biol.* **2014**, *6*, a016295.
- [29] A. D. Luster, P. Leder, *J. Exp. Med.* **1993**, *178*, 1057.
- [30] R. E. Lanford, B. Guerra, D. Chavez, L. Giavedoni, V. L. Hodara, K. M. Brasky, A. Fosdick, C. R. Frey, J. Zheng, G. Wolfgang, R. L. Halcomb, D. B. Tumas, *Gastroenterology* **2013**, *144*, 1508.
- [31] P. J. Pockros, D. Guyader, H. Patton, M. J. Tong, T. Wright, J. G. McHutchison, T.-C. Meng, *J. Hepatol.* **2007**, *47*, 174.
- [32] S. Baenziger, M. Heikenwalder, P. Johansen, E. Schlaepfer, U. Hofer, R. C. Miller, S. Diemand, K. Honda, T. M. Kundig, A. Aguzzi, R. F. Speck, *Blood* **2008**, *113*, 377.
- [33] H. Perkins, T. Khodai, H. Mechiche, P. Colman, F. Burden, C. Laxton, N. Horscroft, T. Corey, D. Rodrigues, J. Rawal, J. Heyen, M. Fidock, M. Westby, H. Bright, *J. Clin. Immunol.* **2012**, *32*, 1082.
- [34] E. Kamphuis, T. Junt, Z. Waibler, R. Forster, U. Kalinke, *Blood* **2006**, *108*, 3253.
- [35] G. A. Rabinovich, D. Gabrilovich, E. M. Sotomayor, *Annu. Rev. Immunol.* **2007**, *25*, 267.
- [36] F. Sato-Kaneko, S. Yao, A. Ahmadi, S. S. Zhang, T. Hosoya, M. M. Kaneda, J. A. Varner, M. Pu, K. S. Messer, C. Guiducci, R. L. Coffman, K. Kitaura, T. Matsutani, R. Suzuki, D. A. Carson, T. Hayashi, E. E. W. Cohen, *JCI Insight* **2017**, *2*, e93397.
- [37] T. Spinetti, L. Spagnuolo, I. Mottas, C. Secondini, M. Treinies, C. Rüegg, C. Hotz, C. Bourquin, *Oncolmunology* **2016**, *5*, e1230578.
- [38] N. Nishii, H. Tachinami, Y. Kondo, Y. Xia, Y. Kashima, T. Ohno, S. Nagai, L. Li, W. Lau, H. Harada, M. Azuma, *Oncotarget* **2018**, *9*, 13301.
- [39] X. Sun, J. Suo, J. Yan, *World J. Gastroenterol.* **2016**, *22*, 6362.
- [40] S. Wang, J. Campos, M. Gallotta, M. Gong, C. Crain, E. Naik, R. L. Coffman, C. Guiducci, *Proc. Natl. Acad. Sci. USA* **2016**, *113*, E7240.
- [41] M. E. Wovk, J. A. Trapani, *Microbes Infect.* **2004**, *6*, 752.
- [42] L. Martínez-Lostao, A. Anel, J. Pardo, *Clin. Cancer Res.* **2015**, *21*, 5047.
- [43] L. Chen, B. Tourville, G. F. Burns, F. H. Bach, D. Mathieu-Mahul, M. Sasportes, A. Bensussan, *Eur. J. Immunol.* **1986**, *16*, 767.
- [44] A. Seth, H. Lee, M. Y. Cho, C. Park, S. Korm, J.-Y. Lee, I. Choi, Y. T. Lim, K. S. Hong, *Oncotarget* **2017**, *8*, 5371.
- [45] M. Chan, T. Hayashi, C. S. Kuy, C. S. Gray, C. C. N. Wu, M. Corr, W. Wrasidlo, H. B. Cottam, D. A. Carson, *Bioconjugate Chem.* **2009**, *20*, 1194.
- [46] D. M. Euhus, C. Hudd, M. C. Laregina, F. E. Johnson, *J. Surg. Oncol.* **1986**, *31*, 229.
- [47] K. J. Livak, T. D. Schmittgen, *Methods* **2001**, *25*, 402.